Model-Based Respiratory Motion Compensation in MRgHIFU

Patrik Arnold[1], Frank Preiswerk[1], Beat Fasel[1], Rares Salomir[2], Klaus Scheffler[3], and Philippe Cattin[1]

[1] Medical Image Analysis Center, University of Basel, Switzerland
patrik.arnold@unibas.ch
[2] Radiology Department, University Hospitals of Geneva, Switzerland
[3] Department of Neuroimaging, University of Tuebingen, Germany

Abstract. Magnetic Resonance guided High Intensity Focused Ultrasound (MRgHIFU) is an emerging non-invasive technology for the treatment of pathological tissue. The possibility of depositing sharply localised energy deep within the body without affecting the surrounding tissue requires the exact knowledge of the target's position. The cyclic respiratory organ motion renders targeting challenging, as the treatment focus has to be continuously adapted according to the current target's displacement in 3D space. In this paper, a combination of a patient-specific dynamic breath model and a population-based statistical motion model is used to compensate for the respiratory induced organ motion. The application of a population based statistical motion model replaces the acquisition of a patient-specific 3D motion model, nevertheless allowing for precise motion compensation.

1 Introduction

Focused Ultrasound deposits sharply localised energy in the tissue causing thermal ablation. Precise targeting demands for exact knowledge of the target's position. The compensation of the fitful respiratory organ motion is a challenging task in the treatment of pathological tissue in abdominal organs. If breathing motion is not compensated, the exposure of healthy tissue increases and the thermal dose delivered to the tumour is reduced. Continuous target displacement tracking in 3D space requires accurate spatial and rapid temporal beam refocusing in the range of millimetres and milliseconds, respectively. Any realisation of a real-time target tracking-based dose delivery must thus be able to predict the target's position at some future time in order to compensate for the finite time delay between the acquisition of the current target's position and the mechanical response of the system to change treatment focus.

During sonication the Magnetic Resonance (MR) scan-time is mainly required for the temperature feedback control of the High Intensity Focused Ultrasound (HIFU) system, quantifying the thermal dose given to the tissue in order to guarantee complete coagulation of the tumour. Therefore, not enough MR scan-time is left to track the tumour in 3D. To determine the thermal dose, temperature maps in regular distances around the tumour are acquired. Similarly as proposed in [1], the navigator (pencil beam) feedback information is used to reposition the temperature mapping slice to resolve organ

P. Abolmaesumi et al. (Eds.): IPCAI 2012, LNAI 7330, pp. 54–63, 2012.

displacements. In this work, we propose to use this 1-dimensional navigator feedback information not only to track the current respiratory state, but also to predict the organ's future displacement, e.g. the position of the tumour.

Several approaches have been proposed to track and predict the motion of abdominal organs. Ries *et al.* [1] proposed a real-time tracking method that observes the target on a 2D image plane combined with a perpendicular acquired pencil beam navigator, providing quasi-3D information of the target trajectories. The future 3D target position is then estimated by a Kalman filter. Underlying a regular and stable breathing pattern, the method was tested in phantom experiments and in vivo on ventilated pigs. The accuracy of the approach is not evaluated on ground truth motion data, but by indirectly comparing the temperature maps obtained after 60 seconds of HIFU sonication with and without motion compensation, resulting in higher maximal temperatures in the target area with enabled motion compensation. However, the experiments have neither been evaluated on ground truth data nor under free breathing conditions.

Ruan and Keall [2] proposed a predictor based on Kernel Density Estimation to account for system latencies caused by software and hardware processing. They use 3D motion trajectories of implanted markers to train the predictor in a lower dimensional feature space using Principal Component Analysis (PCA). The prediction is performed in this subspace and mapped back into the original space for the evaluation. The drawback of the method is that only the position of directly observed internal fiducials can be predicted and not of the entire organ.

Only recently, a combination of a pattern matching approach using a static subject-specific model and a population-based statistical drift model for motion-compensated MRgHIFU treatment was described and evaluated on realistic 4DMRI data [3]. While the results are convincing, the acquisition of a patient-specific 3D motion atlas takes several minutes and the processing time is in the range of hours and thus is not acceptable for clinical use. In particular, the multiple volume-to-volume registrations take up to several hours, in which the patient is asked not to move in order to stay aligned with the acquired model.

Preiswerk *et al.* [4] showed, that the displacement of the entire liver can be spatially predicted by tracking three well distributed markers (implanted fiducials) within the liver using a population-based statistical motion model. Based on an exhalation breath-hold scan, accurate prediction is achieved. Dispensing with the need of extensive pretreatment volume imaging and its time consuming 3D non-rigid registration, no attention is payed to a potential system lag, which is essential for real-time tracking. Also this method is based on full 3D motion information of implanted markers.

The main contribution of the presented work is the combination of a patient-specific fast and lightweight respiratory breathing model and a population-based motion model to a novel, completely non-invasive and clinically feasible 3D motion compensation method for MRgHIFU treatments. The proposed method addresses certain weaknesses of the state-of-the-art methods in terms of real-time usage and validation. On the one hand, the completely MR-based respiratory signal is continuously acquired and used to predict the organs future respiratory state in order to bridge the system's time delay between the tracking and treatment of the target. On the other hand, the

population-based motion model is applied to estimate the motion of the unobserved liver, without the need of acquiring a subject-specific 3D motion model.

2 Materials and Methods

For the evaluation of our approach, a realistic MRgHIFU scenario was assumed. During HIFU sonication, the measured information of the pencil beam navigator, *i.e.* the inferior-superior displacement (1D) of the diaphragm, is used as the *breathing signal*. Based on this *breathing signal* a patient-specific respiratory model is created, whereby a temporal prediction of the diaphragm's future position is estimated (Sec. 2.2). Having an estimate of this displacement, the population-based statistical model is used to compute the most likely 3D displacement of the entire liver, further referred as to *reconstruction* (Sec. 2.3).

2.1 Data and Ground Truth

The ground truth data was acquired by 4DMRI, a dynamic 2D MR imaging method capturing the respiratory motion during free breathing [5]. Thanks to the sagittal slice orientation and the interleaved acquisition of data slices and a dedicated so-called *navigator slice* at a fixed position, vascular structures used for the 3D reconstruction of the volumes are visible during complete breathing cycles and can be tracked with minimal out-of-plane motion. 4DMRI sequences of 20 healthy volunteers (mixed sexes, age range: 17-75) were captured. During acquisition sessions of roughly two hours, 20-45 minutes of time-resolved organ motion data was measured. MR volumes consisting of 25-30 slices (120×192 pixel) covering the right liver lobe with a voxel size of $1.4 \times 1.4 \times 4$ mm^3 and with a temporal resolution of 300-400 ms were obtained. The retrospectively reconstructed 3D stacks cover the entire range of observed breathing depths. By means of B-spline-based 3D non-rigid registration [6], dense spatio-temporal vector fields describing the motion between the different respiratory states of the liver are extracted. The first manually segmented liver exhalation stack is taken as reference volume upon which the subsequent 3D stacks are incrementally registered from time-step to time-step. The vector field from the previous step is taken as an initial estimation, significantly speeding up the registration time and making the registration more robust by reducing the chance of getting trapped in a local minima. The resulting vector fields, describing the liver's displacements relative to the reference volume, serve as the basic data for the motion model and its evaluation in cross-validation experiments.

In order to build a statistical model from this data, inter-subject correspondence had to be established. For each subject mechanical corresponding points were manually selected on the reference volume surfaces in order to align the 20 datasets. These points mark the delineations between the superior surface in contact with lung, the anterior and the posterior areas, which slide along the abdominal wall, and the inferior surface. An isotropic grid with 10 mm resolution was placed in the resulting average liver and then transformed to the shape of each of the subjects. This finally gave a set of 20 topologically equivalent 3D liver volumes as well as vector fields describing the motion

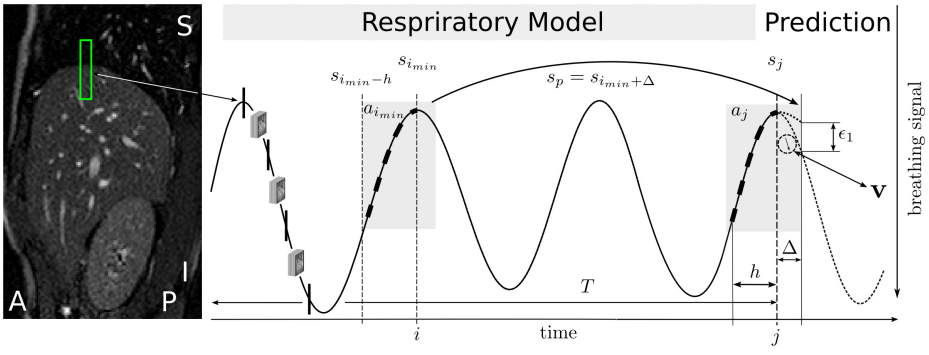

Fig. 1. Schematic illustration of combined respiratory model and motion model-based prediction. Based on the respiratory signal (|) captured at the marked diaphragm region, the displacement s_p of the diaphragm is predicted and from that the full liver displacement $\mathbf{v}$ is *reconstructed*.

for each of the $N = 1261$ inter-subject corresponding grid points. For more detailed information we refer the reader to the article of Preiswerk *et al.* [4].

In this work, the described *breathing signal* is generated by simulating a pencil beam navigator placed on the acquired *navigator slices*. A manually defined region placed anywhere at the diaphragm was persistently tracked by template matching (Normalised Cross Correlation) throughout the acquisition sequence providing one respiratory position and displacement per acquired *navigator slice*, respectively. The inferior-superior component of the templates motion is interpreted as the *breathing signal* as obtained by a common pencil beam navigator, see Figures 1 and 2(a). The spatial resolution is thus given by the image's pixel size of roughly $1.4 \times 1.4\,\mathrm{mm}^2$.

Since the 3D volumes are reconstructed at the time point between two *navigator slices* (see Figure 1, *left*) we linearly interpolate the *breathing signal* in order to obtain the respiratory positions and the 3D volumes at the same time points for the evaluation. In the following we deal with a linearly interpolated *breathing signal* with a sample rate of 6-8 Hz.

2.2 Temporal Prediction

Figure 1 schematically illustrates the prediction scene for the combined patient-specific and population-based model. As described above, the *breathing signal* is extracted by tracking a defined region on all the *navigator slices* followed by linear interpolation obtaining the intermediate respiratory states, where the ground truth 3D data is available for the validation.

The temporal prediction of the *breathing signal* is necessary in order to compensate for the system lag, caused by the pencil beam acquisition time, the processing of the data and the time for refocusing the HIFU beam to the newly calculated target. Any breathing-controlled tracking method must thus be able to estimate the target's position at some future time. The prediction of the future curve of the *breathing signal* is a key part of the prediction pipeline. Faulty predictions lead to wrong assumptions on

the diaphragm's displacement and thus to wrong spatial *reconstructions* of the whole liver displacement. Since the breathing pattern of a free breathing patient is very irregular over time, e.g. the amplitude and phase are changing nearly unpredictably, we use a prediction algorithm which can quickly adapt to the new input data. In the proposed method, however, the tracking of the respiratory state during sonication is based on pencil beams, therefore, one can expect a much lower sampling rate, as for example given by an optical tracking system. In our simulation we deal with a sampling rate of 6-8 Hz. Due to the low sampling rate, the learning based algorithms would lead to considerable prediction errors at each ex- and inhalation position before adapting. Therefore we use a similar technique as proposed in [3], where a one-dimensional breathing model based on the measured pencil beam navigators is created. In contrast to the latter approach where the model is acquired in a training phase and then stays fixed, our respiratory model steadily grows even during increasing treatment time T. Each newly measured data point (pencil beam position) is added to the model, thus getting more and more stable over time. As the prediction algorithm prefers the most recent measurements in the model, the model can be kept small to avoid a system slowdown caused by the increasing model size. All the data stored in the model is observed for the patient-specific operational setup, therefore only realistic displacements of the liver are predicted. For anomalous breathing patterns with a deviation from the breath model above a certain threshold, *i.e.* no matching pattern is found (*e.g.* coughing, new pattern), the HIFU beam can be switched off to ensure patient safety.

The model is best represented by a matrix $\mathbf{A}$, wherein the *breathing signal* is piecewise stored:

$$\mathbf{A} = \left(\begin{array}{cccc|c} s_1 & s_2 & \dots & s_h & s_{h+\Delta} \\ s_2 & s_3 & \dots & s_{h+1} & s_{h+1+\Delta} \\ \vdots & \vdots & & \vdots & \vdots \\ s_{i-h} & s_{i-h+1} & \dots & s_i & s_{i+\Delta} \\ \vdots & \vdots & & \vdots & \vdots \\ s_{T-h} & s_{T-h+1} & \dots & s_T & s_{T+\Delta} \end{array}\right) . \tag{1}$$

The temporal prediction is based on the last h values of the current *breathing signal* given by the vector $\mathbf{a}_j = (s_{j-h}, \dots, s_j)$, where the index j denotes the actual time point. The prediction provides an estimate $s_p = s'_{j+\Delta}$ describing the future signal curve for a later time point, Δ time steps ahead. The best matching pattern of the current *breathing signal* vector $\mathbf{a}_j$ and the column vectors $\mathbf{a}_i$ of $\mathbf{A}$, is found with:

$$i_{min} = \arg\min_i \{ |\mathbf{a}_i - \mathbf{a}_j| \, , \, |j - T| \} \, . \tag{2}$$

The future curve of $\mathbf{a}_{i_{min}}$ with minimum aberration from the actual signal's history $\mathbf{a}_j$ is considered as best estimate of the organ's future respiratory state:

$$s_p = s_{i_{min}+\Delta} \, . \tag{3}$$

The resulting prediction error ϵ_1 is then given by:

$$\epsilon_1 = |s_{j+\Delta} - s_p| \, . \tag{4}$$

The value s_p is the predicted shift in inferior-superior direction of the next diaphragm position. This displacement serves as the input to the motion model that then predicts the position of the entire liver. As the algorithm is continuously adjusting to new input data and updated with the new measured signal input, it can quickly adapt to the irregularity of the periods and amplitudes of the respiratory signal of a free breathing person. Figure 2(b) shows 60 seconds of robust 170 ms ahead prediction performance of an irregular breathing pattern measured by template matching (*blue*) and the model-based prediction (*green*) of subject 4.

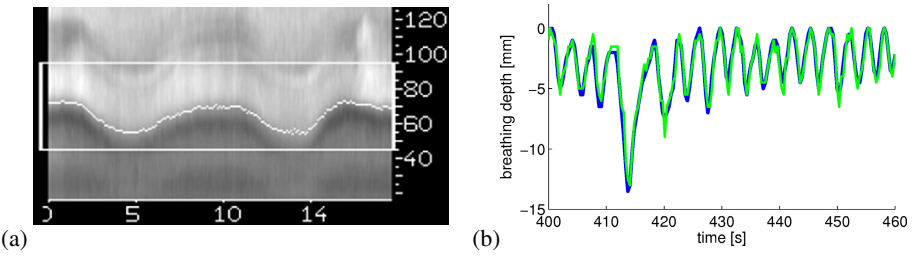

Fig. 2. (a) Typical pencil-beam navigator for MR thermometry real-time slice correction acquired at 10 Hz. (b) Example of 170 ms ahead prediction of a irregular breathing pattern of subject 4. Blue: tracked *breathing signal*; Green: robust respiratory model-based prediction.

2.3 Statistical Modelling

So far, the displacement of only one single point at the diaphragm is known from the prediction. The observed region, the centre of the pencil beam navigator template located on the *navigator slice*, respectively, has to be adopted to the closest grid-point of the subject's liver. The predicted shift s_p is then rigidly assigned to the corresponding model grid-point and the population-based statistical model is used for the *reconstruction* of the entire non-rigid liver displacement. From each of the 20 subjects, the vector fields of the first 15 breathing cycles are taken to build the model. The liver displacements are represented by a $3N$-dimensional vector $\mathbf{v} = (\Delta u_1, \Delta v_1, \Delta w_1, \ldots, \Delta u_N, \Delta v_N, \Delta w_N)'$. Note, that the difference vector $\mathbf{v}$ contains no shape information, but only the relative displacements with respect to the reference volume. The vector fields are mean-free concatenated in a data matrix $\mathbf{X} = (\mathbf{x}_1, \mathbf{x}_2, \ldots, \mathbf{x}_m) \in \mathbb{R}^{3N \times m}$ with $\mathbf{x}_k = \mathbf{v}_k - \bar{\mathbf{v}}$ and sample mean $\bar{\mathbf{v}} = \frac{1}{m} \sum_{k=1}^{m} \mathbf{v}_k$. Applying PCA to the data, the vectors $\mathbf{x}$ are defined by the coefficients c_k and the Eigenvectors $\mathbf{s}_k$ of $\mathbf{S} = (\mathbf{s}_1, \mathbf{s}_2, \ldots)$ of the covariance matrix of the data:

$$\mathbf{x} = \sum_{k=1}^{m-1} c_k \sigma_k \mathbf{s}_k = \mathbf{S} \cdot \mathrm{diag}(\sigma_k)\, \mathbf{c}\,. \tag{5}$$

Hereby, $\sigma_\mathbf{k}$ are the standard deviations within the data along each eigenvector s_k . As elaborated in [7], the model coefficient $\mathbf{c}$ for the full vector $\mathbf{x}$ can be found by an incomplete estimate $s_p \in \mathbb{R}^l, l < N$ that minimises

$$E(\mathbf{c}) = ||\mathbf{Q}\mathbf{c} - s_p|| + \eta \cdot ||\mathbf{c}||^2\,, \tag{6}$$

with $\mathbf{Q} = \mathbf{LS} \cdot \mathrm{diag}(\sigma_k)$, where $\mathbf{L}$ represents a subspace mapping $\mathbf{L} : \mathbb{R}^N \mapsto \mathbb{R}^l$. In the case of a noisy or incorrect assumption s_p, tuning the regularisation factor η allows for *reconstructions* closer to the average quantified by the Mahalanobis distance $||\mathbf{c}||^2$. Solving Eq. 6 for $\mathbf{c}$ with the singular value decomposition of $\mathbf{Q} = \overline{\mathbf{V}}\mathbf{W}\mathbf{V}^T$, yields:

$$\mathbf{c} = \mathbf{V}\,\mathrm{diag}(\frac{w_k}{w_k^2 + \eta})\,\overline{\mathbf{V}}^T s_p\,. \tag{7}$$

Using Eq. 7 the most probable organ displacement under the constraint of the known one-dimensional point-shift prediction s_p is then given by:

$$\mathbf{v} = \mathbf{S} \cdot \mathrm{diag}(\sigma_k)\,\mathbf{c} + \bar{\mathbf{v}}\,. \tag{8}$$

The elaborated framework allows to associate the rigid 1D shift of 1 point placed at the diaphragm with the non-rigid 3D motion of the entire liver based on population statistics.

3 Experiments and Results

To evaluate the prediction performance of the algorithm for clinical relevant motion compensation, experiments on 20 volunteer subjects were performed. On average, displacements of the diaphragm from 5.5 mm to 15.2 mm in inferior-superior direction depending on the subject were observed. For simplicity of generating population statistics, the same amount of data from each subject was included for the experiments. For each experiment 1500 time steps, corresponding to 7-11 minutes, have been predicted.

In a first step, the prediction performance of the respiratory model is tested and evaluated on each of the subjects. In a second step, the respiratory model and the motion model prediction are evaluated in combination with cross-validation experiments. The predictive scene was evaluated every 300-400 ms, at the time points where the ground truth 3D data is available. All experiments were performed with a lookahead length of $\Delta = 1$, *i.e.* 150-200 ms and based on a signal history length of $h = 4$, corresponding to roughly 0.7 s.

3.1 Breath Prediction

Theoretically, the algorithm is able to predict after the first $h = 4$ time steps (≈ 0.7 s). But as more breathing cycles are collected in the respiratory model the more robust the method is predicting. Therefore, we observed the behavior of predictive performance as a function of time, *i.e.* with an increasing model size. Figure 3(a) shows the average error cumulated up to the given time on the axis and error bars showing the standard deviation. The error in prediction is retrospectively computed according to Eq.(4).

In Figure 3(b) the overall results of breath prediction for all 20 subject are visualised by error bars, marking the average and standard deviations. The experiments are evaluated after a model acquisition time of 60 seconds. The average error over all subjects is 0.6 mm with an observed average breathing depth of 8.4 mm.

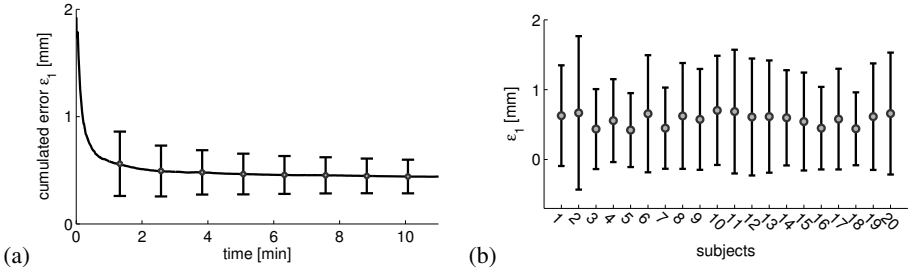

Fig. 3. (a) Average and standard deviations of the cumulated breath prediction error averaged over all subjects. The performance stabilises after a few minutes and is acceptable after 60 seconds. (b) Prediction performance of the respiratory model evaluated for 20 subjects averaged over a prediction length of 7-11 minutes, whereby the first 60 seconds are used to acquire a minimal model. The results are presented by error bars, marking the average and standard deviations for lookahead time of $\Delta_t \approx 180$ ms and signal history length of $h_t \approx 0.7$ s with an overall error of 0.6 mm.

3.2 Motion Model Prediction

The minimum size of population data to create a reliable model is still a unsolved problem as the exact distribution of the data for the entire population is unknown. The suitability of statistical models can, however, be shown empirically in cross-validation experiments. For the evaluation of our motion prediction technique leave-one-out statistical models of all the 20 subjects were computed. From the left-out data a respiratory signal was generated and used as test signal. As explained in Section 2.2 and 2.3, the respiratory motion of the full liver is predicted from one single point at the diaphragm only. For the *reconstruction* we took the 9 first principal components ending up with a model covering 98% of the variance of the original motion data. For each subject the manual segmentation of a reference volume and establishing correspondence (Sec. 2.1) is necessary.

As the predicted shift s_p can not fully be accounted for, the regularisation factor of Eq. (7) was set to $\eta = 5.5$ in order to get more plausible *reconstructions*. The error of prediction is determined by the point-wise Euclidean distance from the predicted liver motion to the ground truth motion of the left-out liver. To give an overview of the error distribution the results are visualised in Figure 4(a) by the median and error bars marking the 25th and 75th percentiles. The dashed line is set to 2 mm, marking an acceptable accuracy limit for HIFU treatments [8]. The average error over all subjects is 1.7 mm, in contrast to the average error without any motion compensation of 3.8 mm. In the case of no motion compensation, the error equals to the mean of the Euclidean distances to the reference volume over time. The spatial distribution of the averaged error over all subjects and time steps is shown in Figure 4(b). The root cause of the error are false predictions in inferior-superior and anterior-posterior direction with a maximal error of 2 mm, 1.1 mm and a minor error in left-right direction of 0.4 mm, respectively.

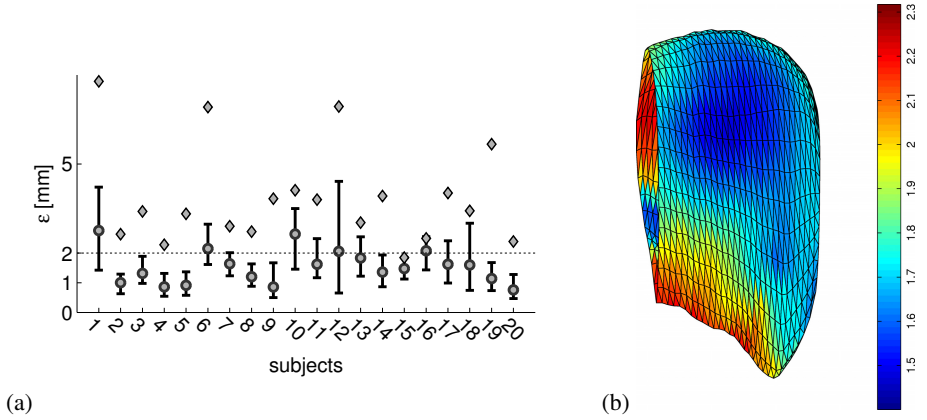

(a) (b)

Fig. 4. (a) Resulting deviations between predicted and ground truth liver motions for 20 different subject over a time interval of 7-11 minutes. Error bars around the median show the 25th and 75th percentile deviation and mean error without any motion compensation (◊). (b) Averaged liver surface from 20 subjects of the right liver lobe at exhalation in anterior view. The colors represent the motion prediction error (in *mm*) averaged over 20 subjects at the liver's surface.

4 Conclusion

We presented a completely non-invasive and purely MR-based tracking method to predict the liver's 3D motion in real-time under free breathing. The method is a combination of a pattern matching approach to predict the patient-specific breathing pattern and a population-based statistical motion model based on PCA to *reconstruct* the respiratory induced organ motion. In the presented work, we demonstrate a safe and efficient technique for MRgHIFU treatment of pathological tissue in moving organs. Although the prediction technique is evaluated on real 4DMRI motion data of the liver, the proposed generic framework is applicable to any abdominal organ, *e.g.* the kidney. The method is evaluated on 4DMRI datasets of 20 healthy volunteers achieving an overall prediction error of 1.7 mm, where the predictive method is clinically applicable after 60 seconds.

Although the overall prediction error of our novel method is slightly higher than the state-of-the-art methods, the proposed technique addresses important issues for the non-invasive real-time application of MRgHIFU treatment in moving abdominal organs. Preiswerk *et al.* [4] achieve a prediction error of 1.2 mm by accurately knowing the 3D displacements of three well distributed points within the liver (*e.g.* implanted surrogate markers). In [3] a prediction error of 1.1 mm is achieved by acquiring 3D information of the patient specific liver motion.

In this work, however, a non-invasive MR-based tracking method is used, allowing to measure the 1-dimensional displacement of a single point on the diaphragm only. We are fully aware of that the second order organ deformation occurring over large time scales, the so called drifts, are not detectable by measuring a single point at the diaphragm only. But, since we are predicting over a short period of time, the different

respiratory states of the liver can reliable be tracked, as has been shown in [9]. Besides a 3D exhalation breath-hold scan, no patient-specific 3D motion data has to be acquired and processed in a pretreatment phase.

In future work we will investigate the possibility of better adapting the population-based motion model to a specific subject. Using a fast MR acquisition sequence, we plan on better restricting the population-based statistical motion model to a specific patient.

Acknowledgments. This work has been supported by the research network of the Swiss National Science Foundation-Project Nr. CR32I3_125499.

References

1. Ries, M., de Senneville, B.D., Roujol, S., Berber, Y., Quesson, B., Moonen, C.: Real-Time 3D Target Tracking in MRI Guided Focused Ultrasound Ablations in Moving Tissues. Magnetic Resonance in Medicine 64, 1704–1712 (2010)
2. Ruan, D., Keall, P.: Online Prediction of Respiratory Motion: Multidimensional Processing with Low-Dimensional Feature Learning. Physics in Medicine and Biology 55, 3011–3025 (2010)
3. Arnold, P., Preiswerk, F., Fasel, B., Salomir, R., Scheffler, K., Cattin, P.C.: 3D Organ Motion Prediction for MR-Guided High Intensity Focused Ultrasound. In: Fichtinger, G., Martel, A., Peters, T. (eds.) MICCAI 2011, Part II. LNCS, vol. 6892, pp. 623–630. Springer, Heidelberg (2011)
4. Preiswerk, F., Arnold, P., Fasel, B., Cattin, P.C.: A Bayesian Framework for Estimating Respiratory Liver Motion from Sparse Measurements. In: Yoshida, H., Sakas, G., Linguraru, M.G. (eds.) Abdominal Imaging. LNCS, vol. 7029, pp. 207–214. Springer, Heidelberg (2012)
5. von Siebenthal, M., Szekely, G., Gamper, U., Boesiger, P., Lomax, A., Cattin, P.: 4D MR Imaging of Respiratory Organ Motion and its Variability. Phys. in Med. Biol. 52, 1547–1564 (2007)
6. Rueckert, D., Sonoda, L.I., Hayes, C., Hill, D.L.G., Leach, M.O., Hawkes, D.J.: Nonrigid Registration Using Free-Form Deformations: Application to Breast MR Images. Transactions on Medical Imaging 18, 712–721 (1999)
7. Blanz, V., Vetter, T.: Reconstructing the Complete 3D Shape of Faces from Partial Information. Informationstechnik und Technische Informatik 44, 295–302 (2002)
8. Vedam, S., Kini, V.R., Keall, P.J., Ramakrishnan, V., Mostafavi, H., Mohan, R.: Quantifying the Predictability of Diaphragm Motion During Respiration with a Noninvasive External Marker. Med. Phys. 30, 505–513 (2003)
9. von Siebenthal, M., Székely, G., Lomax, A.J., Cattin, P.C.: Systematic Errors in Respiratory Gating due to Intrafraction Deformations of the Liver. Med. Phys. 34, 3620–3629 (2007)